

## ON THE DIVERSITY OF THE TAURUS TRANSITIONAL DISKS: UX TAURI A AND LkCa 15

C. ESPAILLAT,<sup>1</sup> N. CALVET,<sup>1</sup> P. D’ALESSIO,<sup>2</sup> J. HERNÁNDEZ,<sup>1,3</sup> C. QI,<sup>4</sup> L. HARTMANN,<sup>1</sup> E. FURLAN,<sup>5,6</sup> AND D. M. WATSON<sup>7</sup>

Received 2007 August 6; accepted 2007 October 11; published 2007 October 29

### ABSTRACT

The recently recognized class of “transitional disk” systems consists of young stars with optically thick outer disks but inner disks which are mostly devoid of small dust grains. Here we introduce a further class of “pre-transitional disks” with significant near-infrared excesses which indicate the presence of an optically thick inner disk separated from an optically thick outer disk; thus, the spectral energy distributions of pre-transitional disks suggest the incipient development of disk gaps rather than inner holes. In UX Tau A, our analysis of the *Spitzer* IRS spectrum finds that the near-infrared excess is produced by an inner optically thick disk and that a gap of  $\sim 56$  AU is present. The *Spitzer* IRS spectrum of LkCa 15 is suggestive of a gap of  $\sim 46$  AU, confirming previous millimeter imaging. In addition, UX Tau A contains crystalline silicates in its disk at radii  $\geq 56$  AU which poses a challenge to our understanding of the production of this crystalline material. In contrast, LkCa 15’s silicates are amorphous and pristine. UX Tau A and LkCa 15 increase our knowledge of the diversity of dust clearing in low-mass star formation.

*Subject headings:* accretion, accretion disks — circumstellar matter — stars: formation — stars: pre-main-sequence

*Online material:* color figures

### 1. INTRODUCTION

Previous studies have revealed stars with inner disks that are mostly devoid of small dust grains, and these “transitional disks” have been proposed as the bridge between Class II objects, young stars surrounded by full disks accreting material onto the central star, and Class III objects, stars where the protoplanetary disk is mostly dissipated and accretion has stopped (e.g., Strom et al. 1989; Skrutskie et al. 1990; Stassun et al. 2001).

New spectra from the *Spitzer Space Telescope* which greatly improve our resolution in the infrared have been used to define the class of “transitional disks” as those with spectral energy distributions (SEDs) characterized by a significant deficit of flux in the near-infrared relative to optically thick full disks, and a substantial infrared excess in the mid- and far-infrared. Extensive modeling studies of several transitional disks around T Tauri stars (D’Alessio et al. 2005; Uchida et al. 2004; Calvet et al. 2005; Espaillat et al. 2007) and F-G stars (Brown et al. 2007) have been presented. In particular, the SEDs of the transitional disks of the T Tauri stars (TTSs) CoKu Tau/4 (D’Alessio et al. 2005), TW Hya (Calvet et al. 2002; Uchida et al. 2004), GM Aur, DM Tau (Calvet et al. 2005), and CS Cha (Espaillat et al. 2007) have been explained by modeling the transitional disks with truncated optically thick disks with most of the mid-infrared emission originating in the inner edge or “wall” of the truncated disk. In all these cases, except for CoKu Tau/4, material is accreting onto the star, so gas remains

inside the truncated disk, but with a small or negligible amount of small dust grains, making these regions optically thin.

Here we present models of UX Tau A and LkCa 15, low-mass pre-main-sequence stars in the young,  $\sim 1$  Myr old Taurus star-forming region which have been previously reported as transitional disks (Furlan et al. 2006; Bergin et al. 2004). We present evidence for gaps in optically thick disks, as opposed to “inner holes”, that is, large reductions in small dust grains from the star out to an outer optically thick wall.

### 2. OBSERVATIONS AND DATA REDUCTION

Figures 1 and 2 are plots of the SEDs for UX Tau A and LkCa 15, respectively. For LkCa 15, the reduction of the *Spitzer* Infrared Array Camera (IRAC) images (program 37) was done with SSC pipeline S14.0 and the post-BCD (Basic Calibrated Data) MOPEX version 030106 (Makovoz et al. 2006). We extracted the photometry of this object using the `apphot` package in IRAF, with an aperture radius of 10 pixels and a background annulus from 10 to 20 pixels. Fluxes at 3.6, 4.5, 5.8, and 8.0  $\mu\text{m}$  are 7.55, 7.35, 7.24, and 6.41 mag ( $1\sigma = 0.05$  mag) calibrated according to Reach et al. (2006). The Submillimeter Array (SMA) observations of LkCa 15 were made on 2003 September 6 using the Compact Configuration of six of the 6 m diameter antennas at 345 GHz with full correlator bandwidth of 2 GHz. Calibration of the visibility phases and amplitudes was achieved with observations of the quasars 0423-013 and 0530+135, typically at intervals of 20 minutes. Observations of Uranus provided the absolute scale for the flux density calibration, and the uncertainties in the flux scale are estimated to be 20%. The data were calibrated using the MIR software package.<sup>8</sup> Fluxes at 216.5, 226.5, 345.2, and 355.2 GHz are  $121.4 \pm 4.3$ ,  $152.8 \pm 5.2$ ,  $416.8 \pm 37.6$ , and  $453.1 \pm 48.1$  mJy, respectively.

<sup>1</sup> Department of Astronomy, University of Michigan, 830 Dennison Building, 500 Church Street, Ann Arbor, MI 48109; ccespa@umich.edu, ncalvet@umich.edu, hernandj@umich.edu, lhartm@umich.edu.

<sup>2</sup> Centro de Radioastronomía y Astrofísica, Universidad Nacional Autónoma de México, 58089 Morelia, Michoacán, Mexico; p.dalessio@astro.unam.mx.

<sup>3</sup> Centro de Investigaciones de Astronomía, Merida 5101 – A, Venezuela.

<sup>4</sup> Harvard-Smithsonian Center for Astrophysics, 60 Garden Street, Cambridge, MA 02138; cqi@cfa.harvard.edu.

<sup>5</sup> NASA Astrobiology Institute, and Department of Physics and Astronomy, UCLA, Los Angeles, CA 90095; furlan@astro.ucla.edu.

<sup>6</sup> NASA Postdoctoral Fellow.

<sup>7</sup> Department of Physics and Astronomy, University of Rochester, Rochester, NY 14627-0171; dmw@astro.pas.rochester.edu.

<sup>8</sup> See <http://www.cfa.harvard.edu/~cqi/mircook.html>.

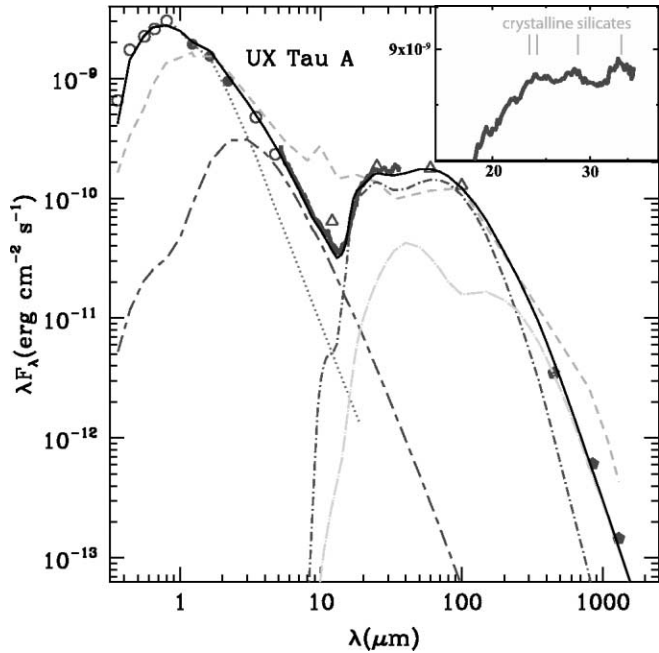


FIG. 1.—SED and model of UX Tau A. We show ground-based optical,  $L$ -, and  $M$ -band photometry (Kenyon & Hartmann 1995; *open circles*);  $J$ ,  $H$ ,  $K$  (2MASS; *filled circles*); *Spitzer* IRS (Furlan et al. 2006; *solid line*); IRAS (Weaver & Jones 1992; *open triangles*); and millimeter (Andrews & Williams 2005; *filled pentagons*) data. The solid black line is the best-fit model with a disk gap of  $\sim 56$  AU (see Table 1 for model parameters). Separate model components are as follows: stellar photosphere (*dotted line*), inner wall (*short-long-dashed line*), outer wall (*dot-short-dashed line*), and outer disk (*dot-long-dashed line*). We also show the median SED of Taurus (*short-dashed line*). The inset is a close-up of the *Spitzer* IRS spectrum longward of  $\sim 16$   $\mu\text{m}$  and indicates the crystalline silicate emission features in addition to underlying features from amorphous silicates (Watson et al. 2007; B. Sargent et al., in preparation). [See the electronic edition of the *Journal* for a color version of this figure.]

### 3. ANALYSIS

#### 3.1. Model Parameters

We follow D’Alessio et al. (2005, 2006) to calculate the structure and emission of the optically thick disk and the wall. Input parameters for the optically thick disk are the stellar properties, the mass accretion rate of the disk ( $\dot{M}$ ), the viscosity parameter ( $\alpha$ ), and the settling parameter  $\epsilon = \zeta_{\text{up}}/\zeta_{\text{st}}$ , i.e., the mass fraction of the small grains in the upper layers relative to the standard dust-to-gas mass ratio (D’Alessio et al. 2006). We use a grain-size distribution that follows a power law of the form  $a^{-3.5}$ , where  $a$  is the grain radius, with a minimum grain size of  $0.005$   $\mu\text{m}$ . In the upper, optically thin layer of the disk, the maximum grain size is  $0.25$   $\mu\text{m}$ . In the midplane of the disk, the maximum grain size is  $1$  mm. The radiative transfer in the wall atmosphere is calculated with the stellar properties,  $\dot{M}$ , the maximum and minimum grain sizes, and the temperature of the optically thin wall atmosphere ( $T_{\text{wall}}$ ). Table 1 lists the maximum grain sizes of the walls and other relevant parameters. We use the same dust composition as Espaillat et al. (2007) unless otherwise noted.

In each case we use a distance of  $140$  pc to Taurus (Kenyon et al. 1994). We assume an outer disk radius of  $300$  AU. Spectral types and stellar temperatures are adopted from Kenyon & Hartmann (1995). Data are dereddened with the Mathis (1990) reddening law, and extinctions are derived from fitting a standard stellar photosphere (Kenyon & Hartmann 1995) to the data. Stellar parameters ( $M_*$ ,  $R_*$ ,  $L_*$ ) are derived from the H-R diagram

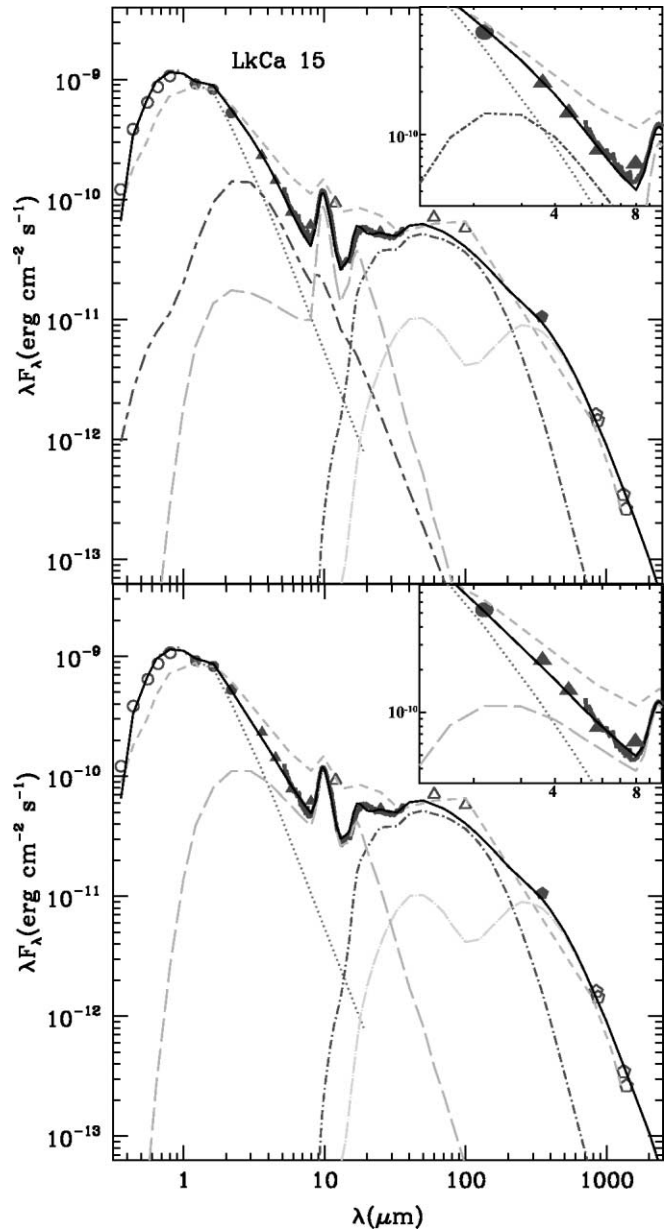


FIG. 2.—SED and model of LkCa 15. Symbols and lines are the same as in Fig. 1. The long-dashed line is the optically thin inner region. Open pentagons come from this work. LkCa 15 has an outer disk that is truncated at an inner radius of  $\sim 46$  AU which is consistent with millimeter results (Piétu et al. 2006). *Top*: We can fit the SED with an inner optically thick wall and a small amount of optically thin dust in the gap. *Bottom*: Here we show a disk model of LkCa 15 without an optically thick inner wall. Model parameters are listed in Table 1. The insets are close-ups of the SED and models between  $3$  and  $\sim 10$   $\mu\text{m}$ . [See the electronic edition of the *Journal* for a color version of this figure.]

and the Baraffe evolutionary tracks (Baraffe et al. 2002). Mass accretion rates are estimated from the  $U$ -band excess following Gullbring et al. (1998) with a typical uncertainty of a factor of  $3$  (Calvet et al. 2004).

#### 3.2. UX Tau A

The sharp flux increase in the SED of UX Tau A (Fig. 1) can be modeled by an optically thick outer disk truncated at  $\sim 56$  AU. The wall of the outer disk dominates the flux in the mid- and far-infrared while the outer optically thick disk contributes to most of the flux in the millimeter. We note that UX

TABLE 1  
STELLAR AND MODEL PROPERTIES

Parameter	UX Tau A	LkCa 15
Stellar Properties		
$M_*$ ( $M_\odot$ )	1.5	1.1
$R_*$ ( $R_\odot$ )	2	1.7
$T_*$ (K)	4900	4350
$L_*$ ( $L_\odot$ )	2.18	0.96
$\dot{M}$ ( $M_\odot \text{ yr}^{-1}$ )	$9.6 \times 10^{-9}$	$2.4 \times 10^{-9}$
Inclination (deg)	60	42 <sup>a</sup>
$A_V$	1.3	1.2
Spectral type	K2	K5
Optically Thick Inner Wall		
$a_{\text{max}}^b$ ( $\mu\text{m}$ )	10	1
$T_{\text{wall}}$ (K)	1400	1400
$z_{\text{wall}}^{b,c}$ (AU)	0.01	0.01
$R_{\text{wall}}$ (AU)	0.16	0.12
Optically Thick Inner Disk <sup>d</sup>		
$R_{\text{disk,outer}}^b$ (AU)	<0.18	<0.15
$M_{\text{disk,inner}}$ ( $M_\odot$ )	$<8 \times 10^{-6}$	$<5 \times 10^{-5}$
Optically Thick Outer Wall		
$a_{\text{max}}$ ( $\mu\text{m}$ )	0.25	0.25
$T_{\text{wall}}^b$ (K)	110	95
$z_{\text{wall}}^b$ (AU)	6	4
$R_{\text{wall}}$ (AU)	56	46
Optically Thick Outer Disk		
$\epsilon^b$	0.01	0.001
$\alpha^b$	0.015	0.0006
$M_{\text{disk}}^b$ ( $M_\odot$ )	0.01	0.1
Optically Thin Inner Region		
$R_{\text{in,thin}}$ (AU)	...	0.15 (0.12) <sup>e</sup>
$R_{\text{out,thin}}^b$ (AU)	...	5 (4)
$a_{\text{min,thin}}$ ( $\mu\text{m}$ )	...	0.005
$a_{\text{max,thin}}$ ( $\mu\text{m}$ )	...	0.25
$M_{\text{dust,thin}}$ ( $M_\odot$ )	...	$4(5) \times 10^{-11}$

<sup>a</sup> Simon et al. (2000).

<sup>b</sup> These are free parameters which are constrained by the best fit to the SED.

<sup>c</sup>  $z_{\text{wall}}$  is the height of the wall above the midplane.

<sup>d</sup> We assume the same  $\epsilon$  and  $\alpha$  as the outer disk.

<sup>e</sup> For LkCa 15, values in parentheses refer to parameters in the case where there is no optically thick inner wall.

Tau A is in a multiple system (Furlan et al. 2006), with the closest component at  $2.6'' \sim 360$  pc in projection; thus, the outer disk may have a smaller  $R_{\text{disk,outer}}$  than assumed here, which may decrease the disk mass but not the derived wall properties  $a_{\text{max}}$ ,  $T_{\text{wall}}$ , and  $z_{\text{wall}}$ , which are constrained by the best fit to the mid-infrared. In modeling the outer disk, we hold  $\dot{M}$  fixed and vary  $\alpha$ ; this is equivalent to finding the best-fit disk mass since  $M_d \propto \dot{M}/\alpha$ .

When compared to the median SED of Taurus (D'Alessio et al. 1999; Furlan et al. 2006, Fig. 1), which has been shown to be representative of an optically thick continuous disk (D'Alessio et al. 1999, 2006), UX Tau A's relatively strong mid-infrared deficit makes it apparent that its disk is not continuous; i.e., it is not a "full disk." However, in contrast with the other transitional disks found around TTSSs, the near-infrared portion of UX Tau A's SED agrees with the median SED of TTSSs in Taurus; this indicates that optically thick material remains in the innermost part of the disk, in contrast to all other transitional disks modeled so far. Since the inner disk is optically thick, it must have a sharp gas-dust transition at the dust destruction radius like that of "full disks" in CTTSSs (Muz-

erolle et al. 2003; D'Alessio et al. 2006). In Figure 1 we show the contribution from the wall of an optically thick inner disk located at the dust destruction radius at 0.16 AU, assuming  $T_{\text{wall}} = 1400$  K. The best fit is obtained with large grains, in agreement with the lack of a  $10 \mu\text{m}$  silicate feature. The flux deficit in the SED around  $10 \mu\text{m}$  puts an upper limit to the extent of the inner optically thick disk at  $<0.18$  AU.

### 3.3. LkCa 15

Our analysis of a model fit to LkCa 15 shows an optically thick disk truncated at  $\sim 46$  AU, as delineated by millimeter interferometric imaging (Piètu et al. 2006). The outer optically thick disk contributes to most of the flux in the millimeter, and the wall of the outer disk contributes much of the flux in the mid- and far-infrared (Fig. 2).

The near-infrared portion of the SED of LkCa 15 lies below the median SED of Taurus, so the case for an optically thick inner disk is not as clear cut as in UX Tau A. However, the near-IR excess above the photosphere in LkCa 15 is substantially higher than is seen in GM Aur (Calvet et al. 2005), TW Hya (Calvet et al. 2002; Uchida et al. 2004), or CS Cha (Espaillat et al. 2007), where the optically thin inner disk contains a small amount of dust. Our analysis suggests that an optically thick inner disk wall at the dust destruction radius (0.12 AU) can account for the significant near-infrared excess in LkCa 15 (Fig. 2, *top*), and that the optically thick component cannot extend beyond 0.15 AU. We also require  $4 \times 10^{-11} M_\odot$  of optically thin dust between 0.15 and 5 AU to produce the  $10 \mu\text{m}$  silicate feature. This optically thin dust mixture is composed of 85% amorphous silicates, 6.8% organics, 1.3% troilite, 6.8% amorphous carbon, and less than 1% enstatite and forsterite. The total emission of this optically thin region is scaled to the vertical optical depth at  $10 \mu\text{m}$ ,  $\tau_0 \sim 0.012$ . We follow Calvet et al. (2002) in calculating the optically thin dust region and note that the dust composition and  $\tau_0$  are free parameters constrained by the best fit to the SED.

In the bottom panel of Figure 2 we present an alternative structure for LkCa 15's inner disk. It is possible to fit LkCa 15's SED with only optically thin dust within the inner hole. In this model, the near-infrared excess and  $10 \mu\text{m}$  emission would originate in  $5 \times 10^{-11} M_\odot$  of optically thin dust located between 0.12 to 4 AU. This optically thin dust mixture would be composed of 61% amorphous silicates, 7% organics, 1% troilite, 30% amorphous carbon, and less than 1% enstatite and forsterite. The total emission of this optically thin region is scaled to the vertical optical depth at  $10 \mu\text{m}$ ,  $\tau_0 \sim 0.018$ . This model (Fig. 2, *bottom inset*) does not fit the slope of the near side of the IRS spectrum ( $<7 \mu\text{m}$ ) or the IRAC data as well as the previously discussed model (Fig. 2, *top inset*). The optical depth in the near-infrared is  $\sim 0.01$ , about 5 times greater than that of the previous model, mainly due to the difference in the amorphous carbon fraction.

While an optically thin region is necessary in both scenarios, we can exclude a model where the optically thin region extends farther than  $\sim 5$  AU since the contribution at  $20 \mu\text{m}$  then becomes too strong.

## 4. DISCUSSION AND CONCLUSIONS

Here we introduce the "pre-transitional disk" class where we see the incipient development of disk gaps in optically thick protoplanetary disks as evidenced by significant near-infrared excesses when compared to the Taurus median SED and previously studied transitional disks (D'Alessio et al. 2005; Calvet

et al. 2002, 2005; Uchida et al. 2004; Espaillat et al. 2007). The pre-transitional disk of UX Tau A has a  $\sim 56$  AU gap as opposed to an inner hole. It is also possible to fit LkCa 15's SED with a  $\sim 46$  AU gap that contains some optically thin dust; a model that has a hole rather than a gap also fits its SED, and future near-infrared interferometry may be able to discriminate between these models. However, the truncation of LkCa 15's outer disk at  $\sim 46$  AU is consistent with resolved millimeter interferometric observations (Piètu et al. 2006), which makes it one of three inner disk holes imaged in the millimeter (TW Hya: Hughes et al. 2007; GM Aur: D. Wilner et al., in preparation). In addition to our sample, the disks around F-G stars studied by Brown et al. (2007) also belong to the pre-transitional disk category. The large gaps that are being detected in pre-transitional disks are most likely due to observational bias since larger gaps will create larger mid-infrared deficits in the SED. Smaller gaps will most likely have less apparent dips in their SEDs and be more difficult to identify; however, if their gaps contain some optically thin material the silicate emission in these objects should be much stronger than can be explained by a full-disk model.

The existence of an inner optically thick disk may be an indicator of the first stages of disk clearing that will eventually lead to the inner holes that have been seen in previously reported transitional disks; this has important implications on disk evolution theories since only planet formation can account for this structure. Hydrodynamical simulations have shown that a newly formed planet could accrete and sweep out the material around it through tidal disturbances and that this is sufficient to produce the hole size in CoKu Tau/4 (Quillen et al. 2004), even maintaining substantial accretion rates (Varnière et al. 2006). Moreover, Najita et al. (2007) have found that the intrinsic properties of transitional disks may favor planet formation. Another proposed formation mechanism for the holes in transitional disks is photoevaporation, in which a photoevaporative wind halts mass accretion toward the inner disk and material in this inner disk is rapidly evacuated, creating an inner hole (Clarke et al. 2001); the hole then increases in size as the edge continues photoevaporating (Alexander & Armitage 2007). Neither this model nor the inside-out evacuation induced by the MRI (Chiang & Murray-Clay 2007) would explain how

an optically thick disk accreting at a sizable accretion rate (see Table 1) would remain inside the hole. Rapid dust growth and settling has also been proposed to explain the holes in disks (Lin & Ida 2004). Again, this does not account for the presence of optically thick inner disk material given that theory suggests grain growth should be fastest in the inner disk, not at some intermediate radius (Weidenschilling 1997; Chiang & Goldreich 1999).

Our sample also has interesting dust compositions (Watson et al. 2007, B. Sargent et al., in preparation). LkCa 15 has an amorphous silicate feature indicating little if any processing leading to the crystallization seen in other young stars. Amorphous silicates are also seen in CoKu Tau/4, DM Tau, and GM Aur (Sargent et al. 2006). In contrast, UX Tau A is different from all the other transitional disks because it has crystalline silicate emission features in addition to amorphous silicate emission features (Fig. 1, *inset*). The wall at  $\sim 56$  AU is the main contributor to the crystalline silicate emission since it dominates the flux in the mid- and far-infrared. This raises the question of whether crystalline silicates are created close to the star or whether they can be created in situ at  $\sim 56$  AU. If the former, it challenges current radial-mixing theories, none of which can get significant amounts of crystalline silicates out to this distance (Gail 2001; Keller & Gail 2004). One possibility for in situ processing may be collisions of larger bodies, which might produce small grains heated sufficiently to create crystals (S. Kenyon 2007, private communication).

Pre-transitional disks offer further insight into the diversity of the "transitional disk" class, and future studies of these disks will greatly advance our understanding of disk evolution and planet formation.

We thank the anonymous referee, E. Bergin, W. Forrest, S. Kenyon, K. H. Kim, J. Miller, B. Sargent, and M. Zhao for insightful discussions. This work is based on observations made with the *Spitzer Space Telescope*. N. C. and L. H. acknowledge support from NASA Origins grants NNG05GI26G and NNG06GJ32G. P. D. acknowledges grants from CONACyT, México. D. M. W. acknowledges support from the *Spitzer* Infrared Spectrograph Instrument Project.

#### REFERENCES

- Alexander, R. D., & Armitage, P. J. 2007, *MNRAS*, 375, 500  
 Andrews, S. M., & Williams, J. P. 2005, *ApJ*, 631, 1134  
 Baraffe, I., et al. 2002, *A&A*, 382, 563  
 Bergin, E., et al. 2004, *ApJ*, 614, L133  
 Brown, J., et al. 2007, *ApJ*, 664, L107  
 Calvet, N., et al. 2002, *ApJ*, 568, 1008  
 ———. 2004, *AJ*, 128, 1294  
 ———. 2005, *ApJ*, 630, L185  
 Chiang, E. I., & Goldreich, P. 1999, *ApJ*, 519, 279  
 Chiang, E. I., & Murray-Clay, R. A. 2007, *Nature Phys.*, 3, 604  
 Clarke, C. J., Gendrin, A., & Sotomayor, M. 2001, *MNRAS*, 328, 485  
 D'Alessio, P., et al. 1999, *ApJ*, 527, 893  
 ———. 2005, *ApJ*, 621, 461  
 ———. 2006, *ApJ*, 638, 314  
 Espaillat, C., et al. 2007, *ApJ*, 664, L111  
 Furlan, E., et al. 2006, *ApJS*, 165, 568  
 Gail, H. P. 2001, *A&A*, 378, 192  
 Gullbring, E., Hartmann, L., Briceño, C., & Calvet, N. 1998, *ApJ*, 492, 323  
 Hughes, A. M., et al. 2007, *ApJ*, 664, 536  
 Keller, Ch., & Gail, H. P. 2004, *A&A*, 415, 1177  
 Kenyon, S. J., Dobrzycka, D., & Hartmann, L. 1994, *AJ*, 108, 1872  
 Kenyon, S. J., & Hartmann, L. 1995, *ApJS*, 101, 117  
 Lin, D. N. C., & Ida, S. 2004, in *ASP Conf. Ser. 323, Star Formation in the Interstellar Medium*, ed. D. Johnstone et al. (San Francisco: ASP), 339  
 Makovoz, D., Khan, I., & Masci, F. 2006, *Proc. SPIE*, 6065, 330  
 Mathis, J. S. 1990, *ARA&A*, 28, 37  
 Muzerolle, J., Calvet, N., Hartmann, L., & D'Alessio, P. 2003, *ApJ*, 597, L149  
 Najita, J. R., Strom, S. E., & Muzerolle, J. 2007, *MNRAS*, 378, 369  
 Piètu, V., et al. 2006, *A&A*, 460, L43  
 Quillen, A. C., et al. 2004, *ApJ*, 612, L137  
 Reach, W., et al. 2006, *Infrared Array Camera Data Handbook*, Ver. 3.0 (Pasadena: Caltech)  
 Sargent, B., et al. 2006, *ApJ*, 645, 395  
 Simon, M., Dutrey, A., & Guilloteau, S. 2000, *ApJ*, 545, 1034  
 Skrutskie, M. F., Dutkevitch, D., Strom, S. E., Edwards, S., Strom, K. M., & Shure, M. A. 1990, *AJ*, 99, 1187  
 Stassun, K. G., Mathieu, R. D., Vrba, F. J., Mazeh, T., & Henden, A. 2001, *AJ*, 121, 1003  
 Strom, K. M., Strom, S. E., Edwards, S., Cabrit, S., & Skrutskie, M. F. 1989, *AJ*, 97, 1451  
 Uchida, K. I., et al. 2004, *ApJS*, 154, 439  
 Varnière, P., Blackman, E. G., Frank, A., & Quillen, A. C. 2006, *ApJ*, 640, 1110  
 Watson, D. M., et al. 2007, *ApJ*, submitted  
 Weaver, W. B., & Jones, G. 1992, *ApJS*, 78, 239  
 Weidenschilling, S. J. 1997, *Icarus*, 127, 290